Optically controlled bistable waveplates

E. Perivolari[a,*], J.R. Gill[b], N. Podoliak[a], V. Apostolopoulos[a], T. J. Sluckin[b], G. D'Alessandro[b], M. Kaczmarek[a]

[a] *Physics and Astronomy, University of Southampton, Southampton SO17 1BJ, United Kingdom*
[b] *Mathematical Sciences, University of Southampton, Southampton SO17 1BJ, United Kingdom*

Abstract

We develop an optically controlled, rewritable half-wave plate based on a twisted nematic liquid crystal cell and present the relevant theory. The cell is bistable, with switching between states controlled by one-step illumination of a single PAAD azobenzene alignment layer with visible light. The photo-alignment properties of the layer enable reversible switching between two perpendicular alignment states at the cell surface, resulting in controllable polarization manipulation. The resulting changes in transmission are observed for four different probe beam wavelengths in the visible and near infrared (NIR) spectral regime. We demonstrate a reproducible modulation of the transmitted polarization with an optical contrast of up to 90-100%. This work represents a first step towards creating LC modulators and phase shifters which can be controlled remotely using only external light sources.

Keywords: Liquid crystals, photoalignment, bistability, optical addressing.

1. INTRODUCTION

Liquid crystals (LCs) lie at the heart of many light-switching devices. Three key properties underlie this capacity. The first is the LC birefringence, the nature of which depends on the relative orientation between the LC molecules and an external electric field. The second is the fact that an external field can also reorient the constituent molecules of a LC (see e.g. [1, 2]). The third is the fact that surface effects, known as anchoring, also orient the LC molecules at the surface, and given orientational molecular interactions, this effect extends into the bulk. Finally, it is usually important to polarize the light both on entering and leaving the cell.

Conventional devices (see e.g. [3, 4]) switch as a result of the imposition of an external voltage, leading to an electric field inside the bulk. The external voltage leads to a reorientation of the LC molecules, which in turn leads to altered optical transmission properties. Informally, one can assert that it is the anchoring effects which conspire to make the reorientation sudden rather than gradual, leading to *switching* rather than mere dimming or brightening.

A disadvantage, at least under some circumstances, of conventional (e.g. 1970s-2000) devices is that their operation requires the continual imposition of a voltage, causing the device to continually consume power. For static displays, in which continual updating is in principle unnecessary, this is a particular problem. It is, however, a problem that can be overcome if the device is constructed so as to be *bistable* (see e.g. [5]). In this case, electric impulses alone should be sufficient to persuade a pixel to switch states.

Constructing a bistable device is no simple matter, though. Take, for example, the now widely used ZBD device [5]. Its operation requires that one of the surfaces be carefully engineered to possess a particular kind of grooves, enabling more than one LC configuration to be stable in the neighborhood of the interface.

In simpler cases, the LC molecules merely align at an interface as the result of surface interactions with an alignment layer. A venerable, if apparently somewhat uncontrolled, technique for creating an alignment layer is to rub the surface with some suitable material [6–8]. This causes the LC molecules in the surface layer to align, usually in the direction of the rubbing, although the mechanism for alignment has been somewhat controversial [9, 10]. There are disadvantages in rubbing for commercial technological applications, and these include the accumulation of static charges, the generation of dust particles [11], and simply the need to incorporate electrodes and an external voltage into the cell design. Furthermore, such surfaces will not, in general, sustain bistability. This would only be possible if the surface alignment can itself be altered, which is completely impractical if the alignment has been achieved by rubbing.

An alternative to the rubbing technique is photopolymerization of an alignment layer. In this method, polarized light is used to align polymer molecules in the surface layer adjacent to the LC [12, 13]. In turn, the surface LC molecules align in accordance with the molecules of the polymer layer. Yuri Reznikov was particularly influential in developing this surface alignment technique, and his name appears on numerous patents and right papers. These date right from the technique's invention in the 1990s (see e.g. [13–18]), and stretch e.g. to his more recent 2012 review with Yaroshchuk [11]. Photoalignment is a much more controlled and reproducible procedure than rubbing, and has the important, extra advantage in the possibility of reorienting a surface layer after a cell's construction. This provides the possibility of bistability without an elabo-

*Author for correspondence - E.Perivolari@soton.ac.uk

rately engineered surface layer, but rather by the ability to reversibly replace one surface orientation with another.

We present a study of a cell with one surface coated with an alignment layer of PAAD-22D, a photoaligning azobenzene dye (from Beam Co.). In general, various different azo-compound materials form films with thickness varying from 20 nm to 500 μm and have been used as photoaligning materials for LCs for the last 30 years [19–25]. PAAD materials have demonstrated themselves to be capable of forming high resolution patterns, enabling their use for polarization gratings and spiral phase wave-plates [26–29], and to be effective in the alignment of LCs [26–32]. They also require low exposure energies and have an absorption spectrum extending past 400 nm [28, 33, 34]. Finally and importantly, it is relatively simple to deposit a PAAD film onto a substrate.

Like all azobenzene-based alignment layers, the molecules of the PAAD-22D layer are able to convert efficiently between their trans and cis states when subject to UV and visible light illumination. The effect of this illumination is similar to that of an electric field in a direction perpendicular to the incident light and its polarization, in that the molecules tend to align along this axis. The mechanism is slightly different to that of an external field, however, which simply rotates the molecules. Rather, according to the 'angular hole-burning model' [31, 35], starting in the thermally stable trans state, the azo-molecules absorb photons and transform into their metastable cis state. They subsequently return, with a random orientation, through either a spontaneous relaxation or a reverse photoisomerization process [30]. The absorption of the photons depends on the angle their electric field makes with the PAAD molecules, with photons absorbed preferentially by molecules parallel to the electric field. It follows that by addressing the PAAD with linearly polarized, visible light for a sufficiently long period of time, the orientation of the PAAD molecules moves towards a population that is entirely perpendicular to the incident electric field (since these are non-absorbing).

In this paper we present the methodology for the construction of optically controlled dynamic half-wave plates, created using the photo-aligning properties of these PAAD materials. Some experimental results for the optical characteristics of the cell are interpreted within the framework of a simple theory. The system can efficiently control the transmission and polarization of light in the visible and NIR region. It is bistable with state-switching achieved by addressing the PAAD layer with visible light, a process that is reversible and reproducible for multiple cycles. In some of our work presented here, the realignment is provided by the probe beam itself. In other experiments, the transmission of a probe beam is monitored, whilst the realignment is carried out by a pump beam at a different wavelength. Our work goes beyond that on previous azo and PAAD systems, where typically, the alignment geometry has been fixed for the duration of the life of the cell, while here the alignment is readdressable.

This paper is organized as follows. In §2 we discuss the experimental setup and the procedure followed to measure the change in the transmittance of the device in both states. We also present a mathematical model and the expected results for the experiment, along with the fitting procedure to model the PAAD realignment dynamics. In §3 we present our results for the transmitted intensity for multiple probe beam wavelengths in the visible and NIR region. This is done for both green and blue pump beams. Finally in §4, we provide a brief discussion of our work and draw some conclusions.

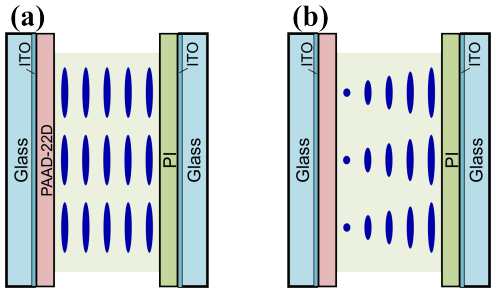

Figure 1: Schematics of a PAAD - LC cell in an (a) planar and (b) twisted bistable state. Switching between (a) and (b) is controlled by one-step illumination with visible light.

2. METHODOLOGY

2.1. Experiment

The nematic LC cell was formed by two glass slides coated with a conductive ITO layer. Both slides received also an additional coating: polyimide (PI) for one, and PAAD-22D for the other, as shown in Fig. 1. The slides were separated by 6.5 μm spacers, and sealed along the perimeter of the cell. The photoalignment layer was prepared by first dissolving commercial PAAD-22D diluted 1% by wt in methanol, and then sonicating the solution for five minutes; a thin film of this solution was spin-coated onto an ITO coated glass substrate. An analogous procedure was followed for the PI layer.

The PI layer was then rubbed to provide a planar alignment in the LC. In order to ensure an initially planar configuration in the LC cell, as shown in Fig. 1(a), the molecules in the PAAD layer were photoaligned to all lie in the same direction; achieved by illuminating them with linearly polarized blue light (λ = 405 nm, E = 0.22 J cm^{-2}). Finally, the cells were filled with the commercially available and widely used nematic LC E7 in the isotropic phase.

Two sets of experiments were carried out, which we will refer to as the single beam and pump-probe experiments. The optical setups are shown in Figs. 2(a) and 2(b), respectively. In all cases, the cell was placed between parallel polarizers (P1 and P2) and a probe beam (B1). The probe was used with a photodiode detector (PD) to determine the LC alignment. The cell was positioned with the initial LC alignment lying vertically. The PAAD-22D photoaligning layer lay on the front face and the PI layer at the far face of the cell. In the single beam experiments, the probe beam (B1) was either green (λ = 532 nm, E = 7.5 J cm^{-2}) or blue (λ = 405 nm, E = 0.22 J cm^{-2}), and had diameter 1 mm. These wavelengths were suitable not only to observe transmission, but also to rotate the easy axis on the PAAD layer surface. The pump-probe experiments involved transmission by either red (λ = 632.8 nm) or NIR

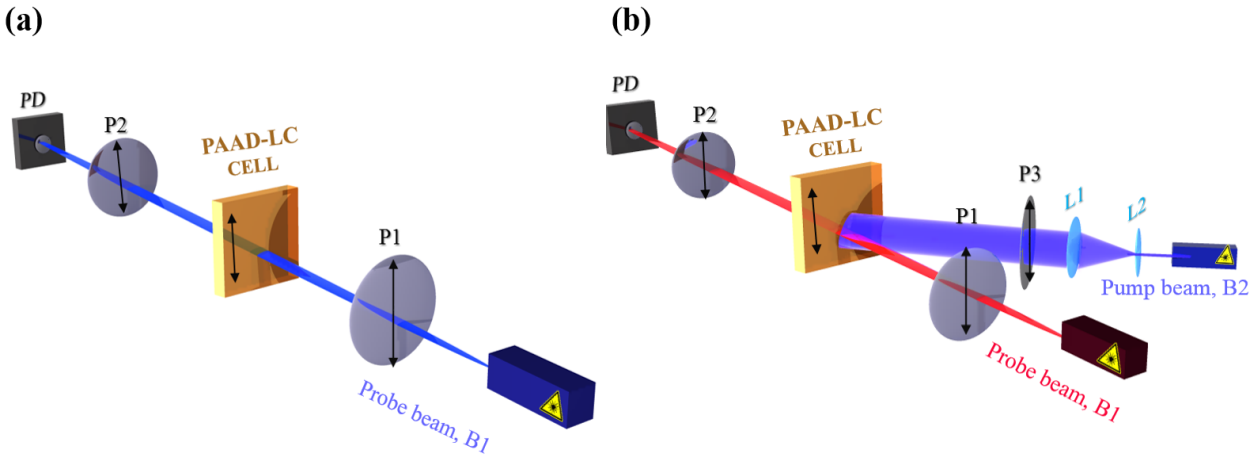

Figure 2: Schematics of the optical setup for the (a) single beam and (b) pump-probe experiments. In both experiments, the PAAD-LC cell is placed between a pair of parallel polarizers (P1 and P2). The alignment is detected by measuring the transmitted intensity of the probe beam (B1) with the photodiode (PD). In the single beam experiments B1 is used also to realign the PAAD layer. In the pump-probe experiments, the pump beam (B2) is used to control the PAAD layer alignment. P3 is the pump beam polariser and L1 and L2 are lenses used to expand the pump beam, if required.

(λ = 808 nm) beams. Light at these wavelengths is not able to rotate the PAAD molecules and the resulting LC surface alignment. In this case, a blue pump beam (B2) with polariser (P3) was used to switch between surface alignments, independently of the probe. In all experiments, the measured transmitted intensity was normalized by taking its ratio with respect to that transmitted through a second planar cell. This second cell was identical to the first in all respects, except for the fact that the PAAD layer had been replaced by a second PI layer. The experimental error of the normalized intensity is 5%. We also monitored the probe power to correct for any fluctuations.

In the single beam experiment, the cell was initially in the planar state, schematically shown in in Fig. 1(a). We have verified the quality of the alignment by checking the cell through cross-polarizers (see the top left panels of figures 3(a) and 3(b). At set times, we inserted a half-wave plate (not shown in figure 2) in front of the laser to rotate its polarization by $\pi/2$ and also rotated P1 by the same amount, causing the polarization of the single beam (B1) to likewise rotate. The polariser P2 followed the polariser P1 so as to remain parallel at all times. Rotating P1 switched the PAAD layer alignment, leading to the $\pi/2$ rotation of the surface alignment that the PAAD layer imposes on the LC. This realigned the LC molecules adjacent to the PAAD layer (hence altering the bulk alignment, also), causing the cell to switch from a planar to a twisted state, shown in in Fig. 1(b). By this same mechanism, subsequent back and forward rotations of P1 and P2 then switched the cell repeatedly between the planar and twisted states.

The experiments consisted of this cycling between planar and twisted states whilst using the photodiode to observe the changing transmission characteristics of the cell as a function of time. In the planar state the transmission is close to unity. In the twisted state the transmission is close to, but not exactly, zero, except when further destructive interference between ordinary and extraordinary beams in the LC cell requires it. Immediately after rotating the polarizers, there is a relaxation process, as the transmission heads towards its new equilibrium. The experiments also involved measuring transmission at different points across the cell.

In the pump-probe experiments the procedure changed. This is because beams at red and NIR wavelengths do not realign PAAD effectively. As a result, the pump beam (B2) and polarizer (P3) were added to the setup. The pump beam was used to address the PAAD layer, with the orientation of P3 dictating the PAAD alignment, and the transmission of the red and NIR probe beams was then measured (in the presence of the pump beam). The diameters of the red and NIR probe beams were 1 and 5 mm, respectively; the corresponding blue pump beam diameters were 1 and 10 mm. The larger pump diameter ensured that the NIR beam probed only the center of the pump beam, ensuring almost uniform alignment. We remark that expanding the pump beam necessarily reduced its intensity, requiring longer, but still experimentally feasible, exposure times for equilibration.

The uniform PAAD reorientation experienced by the expanded beam presented procedural advantages in terms of data analysis. A final experiment returned to the single beam set-up discussed above, but now with the expanded blue beam. This allowed for the study of the realignment dynamics for a beam with a more uniform intensity, as opposed to its original Gaussian profile.

2.2. *Theory*

Twisted cells are normally used in the Mauguin limit, $2\Gamma/\pi \to 0$, with $\Gamma = \frac{2\pi}{\lambda}\Delta n h$. Here λ is the incident light wavelength, Δn the LC birefringence, and h the LC layer thickness. In this limit, the twisted cell rotates the polarization of transmitted light by $\pi/2$ and the transmitted intensity for parallel polarizers P1 and P2 is strictly zero. However, there are corrections to this null result when the ratio is merely small. The Jones matrix approach [4, Ch. 3], yields an expected transmit-

λ/nm	I
405	0.7%
532	1.0%
632	2.1%
808	5.8%

Table 1: Theoretical transmitted intensity $I(\lambda)$ for a $h = 6.5\ \mu$m thick E7 layer in a twisted configuration, see equation (1). The E7 birefringence data was taken from Ref. [36]

ted intensity

$$I(\lambda) = \left(\frac{\pi}{2\Theta}\right)^2 \sin^2\Theta, \tag{1}$$

where

$$\Theta = \left[\frac{\pi^2}{4} + \left(\frac{\Gamma}{2}\right)^2\right]^{\frac{1}{2}}.$$

Substituting the experimental values into (1) yields the values shown in Table 1. From these we can see that in a perfectly twisted configuration, the cells used in our experiments should have an optical contrast that is larger than 99% when probed by green and blue light, and that is about 98% and 94% at the red and NIR wavelengths, respectively.

We also want to be able to determine the dynamics of the PAAD alignment process. We first normalize the transmitted intensity data for the cells with respect to planar and twisted reference cells. These cells are of the same thickness and fabricated using two PI alignment layers. The transmission $I(t)$ is then modeled using the empirical functional form

$$I(t) = b + a_1 e^{-t/\tau_1} + a_2 e^{-t/\tau_2}. \tag{2}$$

The parameter b is the asymptotic intensity, $I(t \to \infty)$. The optical contrast is the difference between the intensities in the twisted and untwisted states. Experimentally this varies slightly from step to step, but it is fairly constant after an initial transient, see Fig. 4(b) and (d).

There are two time constants, $\tau_1 \ll \tau_2$ ("fast" and "slow", respectively). In practice we find that with the expanded pump beam a single time constant suffices. Thus, τ_1 seems to reflect the effect of the joint PAAD-LC dynamics, while τ_2 is a semi-empirical approximation to an average of a multiscale relaxation process over different points in the cell, caused by the non-uniform intensity of the aligning beam. The link between the time constants and the PAAD and LC dynamics, however, remains to be investigated more fully.

3. RESULTS

Fig. 3 shows microscope images of a cell during two cycles of the twist and untwist alignments, addressed with green and blue light, respectively. Each image is taken at a different point in the cell. Step 1 corresponds to the initial planar state, step 2 to the first twisted state, step 3 to the second planar state, and step 4 to the second twisted state. The images are taken with the cell between parallel polarizers; the bright regions correspond to the planar state and dark regions to the twisted state.

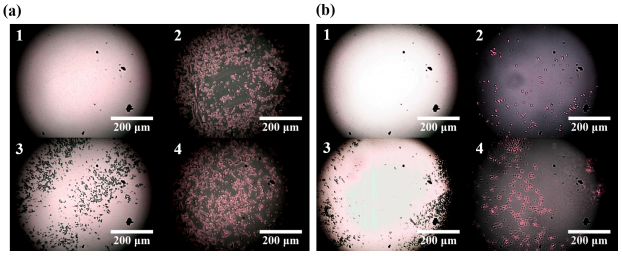

Figure 3: Co-polarized microscope images of cells: Panel (a): aligned with green beam; Panel (b): aligned with blue beam. Within each panel: 1) Initial planar state. 2) First twisted state. 3) Second planar state. 4) Second twisted state.

PAAD illumination	$\tau_1[s]$
Narrow green	46
Narrow blue	5.8
Expanded blue	59

Table 2: Fitted values of the time constant τ_1 for three different types of illumination of the PAAD layer.

The twisting and untwisting was achieved using a single external laser source as described in §2.1. It can clearly be seen that the blue beam provides a better alignment than the green, and that in both cases the structures formed are not completely uniform. Moreover, there is a noticeable, although not dramatic, change between the initial PAAD alignment through a cycle of realignment and subsequent alignment.

We can compare this qualitative analysis with the quantitative analysis in Fig.4. Figs. 4(b) and 4(d) show the degree of alignment in these cycles in both the green and blue beam cases, respectively. The degree of alignment reached in each step seems to be rather similar, but not identical, especially for the first cycle, consistent with the images in Fig. 3. The transmittance of the recovered planar state is up to 70% with green light and up to 90% with blue light (in comparison with the reference planar cell). The contrast ratio is approximately 55% and 80%, respectively. We note that the contrast ratio measurement for the blue beam may be affected by the normalization procedure we have followed: the PAAD layer absorbs part of the blue beam, while its replacement PI layer in the reference cell does not. Therefore, the normalized intensity curves in Fig. 4(c) cannot reach 1 and the contrast ratio measured is an underestimate of the "real" ratio.

A similar picture appears when considering the dynamics, which is presented in Figs. 4(a) and 4(c) for the green and blue beams, respectively. There seems to be a single initial anomalous cycle in which the relaxation process differs from the relaxation processes in subsequent cycles. The relaxation processes in the later cycles repeat reproducibly. We can regard the first anomalous cycle as a transient. The physics of this transient is not yet understood, although we might regard it as being analogous to work-hardening processes in stressed defected alloys. Moreover, the relaxation time is much quicker for the blue beam (compare Figs. 4(a) and (c) and see Table 2). This is to be expected because the blue beam wavelength lies closer to

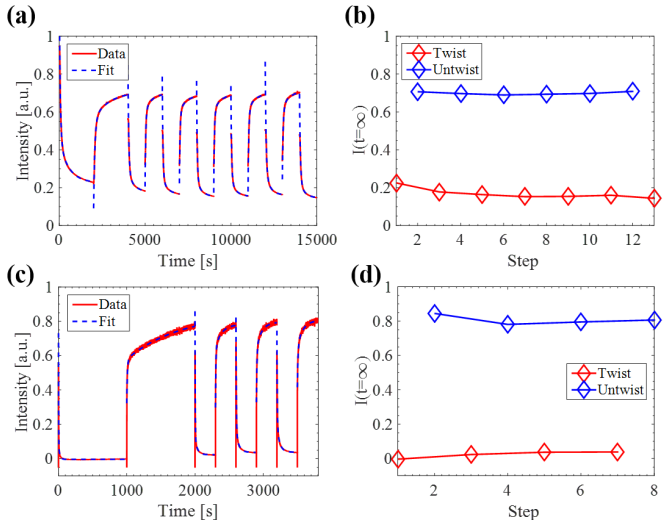

Figure 4: Results of the single beam experiments. The top and bottom rows correspond to green and blue beam illumination respectively; the left column shows the transmitted intensity as a function of time over several cycles; the right column shows the normalized asymptotic illumination intensity (parameter b in equation (2)) of the twisted and untwisted states in subsequent cycles.

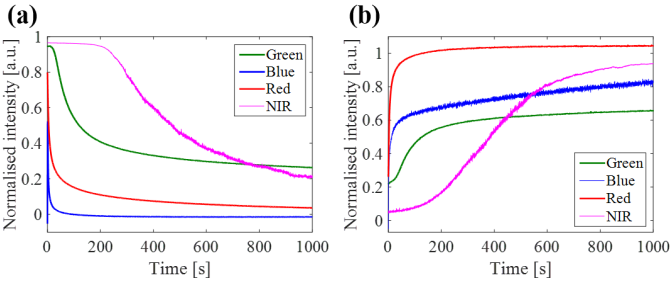

Figure 5: Transmitted intensity against illumination time for a green single beam, blue single beam, blue pump and red probe, and an expanded blue pump and NIR probe. (a) Initial twisting step; (b) Subsequent untwisting. The experimental error of the normalized intensity is 5%, as discussed in §2.1 .

the absorption peak of PAAD-22D. We observed that the same quality of photoalignment could not be achieved by illuminating with a green beam even for extended periods of time. To summarize, these devices are dynamic and switchable with reproducible properties, enabling the control of the transmission and polarization of the probe beam using only an external light source.

The blue beam provides both faster and better quality photoalignment, and was thus used as the photoaligning agent in the pump-probe experiments with red (632.8 nm) and NIR (808 nm) probe beams. Two experiments were carried out, with standard and expanded blue pump beams, respectively. The results of this are shown in Fig. 5. Fig. 5(a) shows the first twisting step and Fig. 5(b) the subsequent untwisting. The equivalent single green and blue beam data are shown for comparison. The NIR data is taken with an expanded blue pump beam, as explained in §2.1. The pump intensity was consequently much reduced and the NIR relaxation process is much slower.

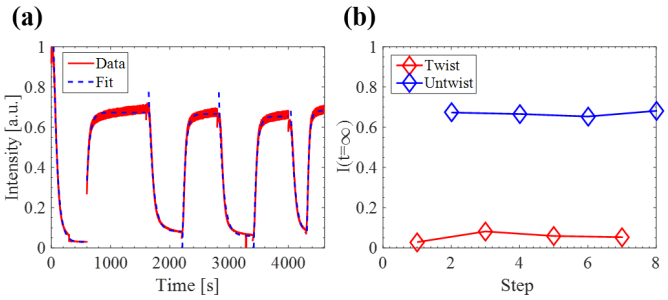

Figure 6: Transmitted intensity against illumination time for an expanded blue beam (a) Relaxation dynamics for the first few twist/untwist cycles. (b) Asymptotic intensities at subsequent twist and untwist steps.

The last experiment to take place used the expanded blue pump beam in the single beam set up. In this case, again, the loss of intensity due to the increased beam size resulted in much longer realignment times (see Fig. 6 and Table 2). Importantly, though, the expanded single blue beam relaxation data could be analyzed using only a single exponential, as opposed to the two needed for the narrow beam experiments. We thus conclude that the second time constant was in fact the result of the difference in intensities, and hence alignment speeds, between the inner and outer beam, due to its Gaussian profile.

The contrast ratio for the red beam is nearly 100% (compare the two red curves in Fig. 5). As the red beam twist is driven by a narrow blue pump beam, this indicates that the measured contrast ratio of the single blue beam experiment is indeed affected by absorption in the PAAD layer, as discussed above in the analysis of Fig. 3. In the NIR beam experiment, the slow time dynamics and problems in maintaining its stability for such long times did not allow us to reach an asymptotic state and measure the contrast ratio.

The slow dynamics caused by the low intensity of the expanded blue beam has left us with two open problems: (*i*) the NIR and expanded blue beam have different dynamics (compare Fig. 5 and 6); (*ii*) the contrast ratio of the expanded blue beam, see Fig. 6(b), is approximately 65%, much lower than the narrow blue beam. Both effects may be due to an interplay between the LC and PAAD dynamics and may also be affected by a poorer realignment of the PAAD layer. Both aspects require further study.

4. CONCLUSIONS AND DISCUSSION

Work previously carried out on PAAD and other azo-based material systems focused on fixed geometries, with UV used to set the alignment. [11]. In this paper we have demonstrated the feasibility of using a PAAD-22D photoalignment layer to fabricate a dynamic system capable of forming rewritable twisted LC structures . The system is all-optically controlled and uses only visible light. There is no requirement for electrodes or an applied field to control the dynamic behavior. In doing so, we were able to create dynamic half-wave plates for efficiently controlling the transmission and polarization of light. The PAAD was addressed with green and blue light, with blue

proving itself to provide much faster and better quality alignments. Addressing the same point of the cell, the transmitted intensity of the initially planar cell was repeatedly recovered to approximately 90% after many twist and untwist steps. We have also demonstrated that, with the use of a blue pump beam, the transmission of both red and NIR probe beams can be modulated selectively, with greater than 90% efficiency in the case of the red beam. However, some puzzles still remain, concerning the precise physics of the relaxation process, the extent of the rewritability, and the anomalous nature of the early cycles of the rewriting process.

Acknowledgments

The authors would like to thank Prof Nelson Tabiryan and his group for their assistance with the material samples and their valuable advice.

Our deepest acknowledgment is to the late Yuri Reznikov. He has been taken from us too young, and it is hard to believe that now instead of merely being far away, he is no longer with us. Yuri's work in LCs in general, and in the context of this paper, in the area of photoalignment of LC surfaces in particular, has been extremely influential. The influence extends from our own group, to the world-wide LC community. Yuri was a direct collaborator (and dare we say it, friend) of four of us (MK, NP, GD and TJS). He was also the PhD supervisor of Oleksandr Buchnev (discussions with whom we also acknowledge), an important collaborator and member of the Southampton LC group, whose skills have been essential in pushing forward our work in recent years. Yuri was always extremely supportive of junior researchers.

We remember with fondness Yuri's visits to Southampton, our visits to his laboratory at the Institute of Physics on Nauki Avenue in Kyiv, and numerous passing interactions at LC conferences across the globe. He was a stimulating intellectual companion, not only when talking about his specialist area, but in general conversation about scientific and cultural topics. And beyond that, he was a genuinely nice man, in a competitive career when often there is a temptation to behave in uncomradely fashion. Even beyond the grave, for many years to come, both Yuri's memory and his scientific influence will long be present in the LC community.

REFERENCES

[1] J. Prost, de Gennes P.-G., The Physics of Liquid Crystals, Clarendon Press, 1995.

[2] I.-C. Khoo, Liquid crystals: physical properties and nonlinear optical phenomena, Vol. 64, John Wiley & Sons, 2007.

[3] L. M. Blinov, V. G. Chigrinov, Electrooptic effects in liquid crystal materials, Springer, 1994.

[4] D. K. Yang, Fundamentals of Liquid Crystal Devices, Wiley Series in Display Technology, Wiley, 2014.

[5] G. P. Bryan-Brown, C. V. Brown, J. C. Jones, Bistable nematic liquid crystal device, US Patent 6,249,332 (2001).

[6] H. Zocher, *Über die optische Anisotropie selektiv absorbierender Stoffe und über mechanische Erzeugung von Anisotropie* (On the optical anisotropy of selectively absorbing materials and the mechanical generation of anisotropy), Naturwissenschaften 13 (1925) 1015–1021.

[7] P. Chatelain, *Sur l'orientation des cristaux liquides par les surfaces frottèes* (On the orientation of liquid crystals by rubbed surfaces), Comptes Rendus de l'Académie de Sciences 213 (1941) 875–76, English translation in *Crystals that Flow* (T.J. Sluckin, D.A. Dunmur and H. Stegemeyer, eds) Taylor and Francis London 2004; pp320-323.

[8] A. A. Sonin, The surface physics of liquid crystals, Taylor & Francis, 1995.

[9] Y. Sato, K. Sato, T. Uchida, Relationship between rubbing strength and surface anchoring of nematic liquid crystal, Japanese Journal of Applied Physics 31 (1992) L579.

[10] E. S. Lee, P. Vetter, T. Miyashita, T. Uchida, Orientation of polymer molecules in rubbed alignment layer and surface anchoring of liquid crystals, Japanese Journal of Applied Physics 32 (1993) L1339–1341.

[11] O. Yaroshchuk, Y. A. Reznikov, Photoalignment of liquid crystals: basics and current trends, Journal of Materials Chemistry 22 (2012) 286–300.

[12] W. M. Gibbons, P. J. Shannon, S.-T. Sun, B. J. Swetlin, Surface-mediated alignment of nematic liquid crystals with polarized laser light, Nature 351 (1991) 49–50.

[13] A. Dyadyusha, V. M. Kozenkov, T. Y. Marusiy, et al., Light-induced planar alignment of nematic liquid-crystal by the anisotropic surface without mechanical texture, Ukrainskii Fizicheskii Zhurnal 36 (1991) 1059–1062.

[14] T. Y. Marusii, Y. A. Reznikov, Photosensitive orientants for liquid crystal alignment, Mol. Mat 3 (1993) 161–168.

[15] D. S. Kang, W. S. Park, H. H. Shin, et al., Method for forming an orientation film of photopolymer in a liquid crystal display, US Patent 5,464,669 (1995).

[16] D. Voloshchenko, A. Khyzhnyak, Y. A. Reznikov, V. Y. Reshetnyak, Control of an easy-axis on nematic-polymer interface by light action to nematic bulk, Japanese journal of applied physics 34 (1995) 566.

[17] W. S. Park, H. H. Shin, S. B. Kwon, et al., Liquid crystal device utilizing thermostable polymeric material, US Patent 5,538,823 (1996).

[18] A. Dyadyusha, A. Khizhnyak, T. Marusii, et al., Peculiarity of an oblique liquid crystal alignment induced by a photosensitive orientant, Japanese journal of applied physics 34 (8A) (1995) L1000–1002.

[19] N. Tsutsumi, Recent advances in photorefractive and photoactive polymers for holographic applications, Polymer International 66 (2017) 167–174.

[20] F. You, M. Y. Paik, M. Häckel, et al., Control and suppression of surface relief gratings in liquid-crystalline perfluoroalkyl–azobenzene polymers, Advanced Functional Materials 16 (2006) 1577–1581.

[21] L. Miccio, M. Paturzo, A. Finizio, P. Ferraro, Light induced patterning of poly (dimethylsiloxane) microstructures, Optics express 18 (2010) 10947–10955.

[22] O. R. Bennani, T. A. Al-Hujran, J.-M. Nunzi, R. G. Sabat, O. Lebel, Surface relief grating growth in thin films of mexylaminotriazine-functionalized glass-forming azobenzene derivatives, New Journal of Chemistry 39 (2015) 9162–9170.

[23] J. Gao, Y. He, F. Liu, et al., Azobenzene-containing supramolecular side-chain polymer films for laser-induced surface relief gratings, Chemistry of Materials 19 (2007) 3877–3881.

[24] S. K. Yesodha, C. K. S. Pillai, N. Tsutsumi, Stable polymeric materials for nonlinear optics: a review based on azobenzene systems, Progress in Polymer Science 29 (2004) 45–74.

[25] O. Francescangeli, S. Slussarenko, F. Simoni, et al., Light-induced surface sliding of the nematic director in liquid crystals, Physical Review Letters 82 (1999) 1855–1858.

[26] L. De Sio, D. E. Roberts, Z. Liao, et al., Digital polarization holography advancing geometrical phase optics, Optics Express 24 (16) (2016) 18297–18306.

[27] S. R. Nersisyan, N. V. Tabiryan, D. Mawet, E. Serabyn, Improving vector vortex waveplates for high-contrast coronagraphy, Optics Express 21 (7) (2013) 8205–8213.

[28] A. Priimagi, A. Shevchenko, Azopolymer-based micro-and nanopatterning for photonic applications, Journal of Polymer Science Part B: Polymer Physics 52 (2014) 163–182.

[29] A. Priimagi, J. Vapaavuori, F. J. Rodriguez, et al., Hydrogen-bonded polymer- azobenzene complexes: Enhanced photoinduced birefringence with high temporal stability through interplay of intermolecular interactions, Chemistry of Materials 20 (2008) 6358–6363.

[30] H. Akiyama, T. Kawara, H. Takada, et al., Synthesis and properties of azo dye aligning layers for liquid crystal cells, Liquid Crystals 29 (2002)

1321–1327.
[31] P.-A. Blanche, P. C. Lemaire, M. Dumont, M. Fischer, Photoinduced orientation of azo dye in various polymer matrices, Optics Letters 24 (1999) 1349–1351.
[32] A. Glushchenko, H. Kresse, V. Y. Reshetnyak, Y. A. Reznikov, O. Yaroshchuk, Memory effect in filled nematic liquid crystals, Liquid crystals 23 (1997) 241–246.
[33] F. P. Nicoletta, D. Cupelli, P. Formoso, et al., Light responsive polymer membranes: a review, Membranes 2 (2012) 134–197.
[34] J. Griffiths, Selected aspects of photochemistry II: Photochemistry of azobenzene and its derivatives, Chemical Society Reviews 1 (1972) 481–493.
[35] M. L. Dumont, S. Hosotte, G. Froc, Z. Sekkat, Orientational manipulation of chromophores through photoisomerization, in: R. A. Lessard (Ed.), Photopolymers and Applications in Holography, Optical Data Storage, Optical Sensors, and Interconnects, SPIE-Intl Soc Optical Eng, 1994, pp. 2–13.
[36] J. Li, C.-H. Wen, S. Gauza, R. Lu, S.-T. Wu, Refractive Indices of Liquid Crystals for Display Applications, IEEE J. Display Tech. 1 (2005) 51–61. doi:10.1109/JDT.2005.853357.